

NGC 7538 IRS 1 - AN IONIZED JET POWERED BY ACCRETION

GÖRAN SANDELL

SOFIA-USRA, NASA Ames Research Center, MS N211-3, Moffett Field, CA 94035, U.S.A.

W. M. GOSS

National Radio Astronomy Observatory, P.O. Box O, Socorro, NM 87801, U.S.A.

MELVYN WRIGHT

Radio Astronomy Laboratory, University of California, Berkeley 601 Campbell Hall, Berkeley, CA 94720, U.S.A.

AND

STUART CORDER¹

Joint ALMA Observatory, Av Apoquindo 3650 Piso 18, Las Condes, Santiago, Chile

Draft version August 11, 2018

ABSTRACT

Analysis of high spatial resolution VLA images shows that the free-free emission from NGC 7538 IRS 1 is dominated by a collimated ionized wind. We have re-analyzed high angular resolution VLA archive data from 6 cm to 7 mm, and measured separately the flux density from the compact bipolar core and the extended (1''5 - 3'') lobes. We find that the flux density of the core is $\propto \nu^\alpha$, where ν is the frequency and α is ~ 0.7 . The frequency dependence of the total flux density is slightly steeper with $\alpha = 0.8$. A massive optically thick hypercompact core with a steep density gradient can explain this frequency dependence, but it cannot explain the extremely broad recombination line velocities observed in this source. Neither can it explain why the core is bipolar rather than spherical, nor the observed decrease of 4% in the flux density in less than 10 years. An ionized wind modulated by accretion is expected to vary, because the accretion flow from the surrounding cloud will vary over time. BIMA and CARMA continuum observations at 3 mm show that the free-free emission still dominates at 3 mm. HCO⁺ J = 1 \rightarrow 0 observations combined with FCRAO single dish data show a clear inverse P Cygni profile towards IRS 1. These observations confirm that IRS 1 is heavily accreting with an accretion rate $\sim 2 \cdot 10^{-4} M_\odot/\text{yr}$.

Subject headings: accretion, accretion disks – H II regions – stars: early-type – stars: formation

1. INTRODUCTION

NGC 7538 IRS 1 was first detected in the radio at 5 GHz by Martin (1973), who found three compact radio sources at the SE edge of the large ($\sim 4'$) H II region NGC 7538, which is at a distance 2.65 kpc (Moscadelli et al. 2008). The brightest of the three, source B, has later become known as IRS 1 (Wynn-Williams, Becklin, & Neugebauer 1974). The far-infrared luminosity of the three sources is $\sim 1.9 \cdot 10^5 L_\odot$, completely dominated by IRS 1 (Hackwell, Grasdalen & Gehrz 1982). IRS 1 was first resolved with the VLA at 14.9 GHz by Campbell (1984), who showed that it has a compact ($\sim 0''.2$) bipolar N-S core with faint extended fan-shaped lobes, suggesting an ionized outflow. This is an extremely well-studied source with numerous masers, a prominent molecular outflow and extremely broad hydrogen recombination lines indicating substantial mass motion of the ionized gas (Gaume et al. 1995; Sewilo et al. 2004; Keto et al. 2008). Although it has been modeled as an ionized jet (Reynolds 1986) or a photo-ionized accretion disk (Lugo, Lizano & Garay 2004), the source is usually referred to as an Ultra Compact or Hyper

Compact H II region with a turnover at ~ 100 GHz. Since we have carried extensive observations of IRS 1 with BIMA and CARMA, the desire to determine the contribution from dust emission at mm-wavelengths led us to investigate where the free-free emission from IRS 1 becomes optically thin. Such a determination is not possible from published data, because IRS 1 has been observed with a variety of VLA configurations, some of which resolve out the extended emission and others may only quote total flux. This prevented us from separately estimating the flux for the compact bipolar core and the extended lobes. Furthermore the flux density varies with time (Franco-Hernández & Rodríguez 2004), which makes it difficult to derive an accurate spectral index.

2. VLA ARCHIVE DATA

We have retrieved and re-analyzed a few key observations of NGC 7538 IRS 1 from the VLA data archive. These are all long integration observations with very high angular resolution, good uv-coverage, and high image fidelity. Table 1 gives the observing dates, synthesized beam width, sensitivity, the integrated flux of the bipolar core, and the observed total flux. We included a BnA array observation obtained by us at X-band (8.5 GHz) (Sandell, Goss & Wright 2005), because it is more contemporary with the high frequency data sets and pro-

Electronic address: Goran.H.Sandell@nasa.gov

¹ Jansky Fellow, NRAO

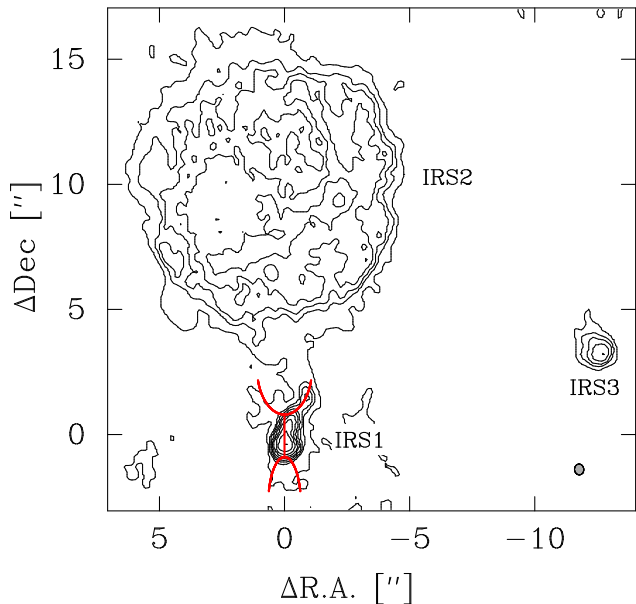


FIG. 1.— C-band (4.8 GHz) image of the IRS1 - 3 field. The beam size is plotted in the bottom right corner of the image. The first contour is at $3\text{-}\sigma$ level, the next contour 3 times higher and from there on we plot 7 logarithmic contours. An outline of the jet from IRS 1, plotted in red, shows the optically thick inner part of the jet and where the jet expands and becomes optically thin. Fig 2 zooms in on the inner optically thick part of the jet and illustrates how the jet becomes smaller when we go up in frequency due to the outer portion of the jet becoming optically thin.

vides an additional data point at a frequency where there are no other high angular resolution VLA data available. Fig 1 shows the IRS 1 - 3 field at 4.8 GHz, while Fig 2 shows the morphology of the compact bipolar core as a function of frequency.

3. ANALYSIS OF VLA DATA

We determined flux densities of the compact bipolar core with an accuracy of a few percent. The results are given in Table 1. Table 1 also gives total flux densities, obtained by integrating over the whole area where we detect emission from IRS 1. At 4.9 GHz the total linear extent of IRS 1 is $\sim 7''$, while it is $\sim 1''.4$ at 43.4 GHz. Even though we can reliably determine the flux density of the bipolar core at 43.4 GHz, some of the faint extended emission is filtered out; therefore the total flux is underestimated. At 4.9 GHz the bipolar core has a total length of $\sim 1''.1$ FWHM (Full Width Half Maximum), with a separation between the two peaks of $0''.68$, at 14.9 GHz the size is $0''.44$ with a peak separation of $0''.24$ (Table 1). At 43.4 GHz we can still fit the core with a double Gaussian with a peak separation of $\sim 0''.12$, while the linear size (length) has a FWHM of $0''.20$. Since one of our data sets (X-band, 8.4 GHz) has insufficient resolution to resolve the two bipolar cores, we plot the linear size (length) as a function of wavelength in Fig. 3, although fitting to the lobe separation gives virtually identical results, but with a larger uncertainty. We find the size to vary with frequency as $\nu^{-0.8 \pm 0.03}$, while the flux density increases with frequency as $\nu^{0.7 \pm 0.05}$. The frequency dependence of the total flux is more difficult to estimate, since some VLA configurations are not very sensitive to faint extended emission and will therefore underestimate the total flux. If we chose data sets which give a reliable

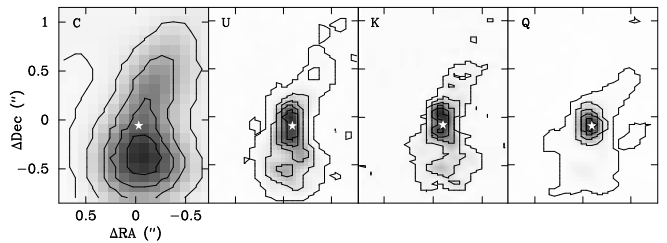


FIG. 2.— VLA images at 4.86, 14.94, 22.37, & 43.37 GHz showing the bipolar core surrounding IRS 1. Beam sizes are given in Table 1. The C-band image (Fig. 1) shows faint extended lobes extending several arcseconds to the north and south of IRS 1. These images show that the core shrinks in size with increasing frequency.

flux for IRS 2², which is a spherical H II region with a size of $\sim 8''$, we find that the total flux from IRS 1 has a slightly steeper spectral index, 0.8 ± 0.03 determined from data sets from 4.8 GHz to 49 GHz. The fit to the total flux densities for IRS 1 is shown as a dotted line in Fig. 3. Such a shallow frequency dependence would require a very steep density gradient in the ionized gas, if the emission originates from an H II region ionized by a central O-star, although it is not impossible, see e.g. Keto et al. (2008). A high-density H II region with a steep density gradient should be spherical, not bipolar with a dark central lane as we observe in IRS 1. Neither can a steep density gradient model explain the extremely broad recombination lines observed in IRS 1 (Gaume et al. 1995; Keto et al. 2008). All these characteristics can be explained, if the emission originates in an ionized stellar wind or jet (Reynolds 1986). The inner part of the jet is optically thick and further out, where the jet expands, the emission becomes optically thin. At higher frequencies the outer part of the jet becomes optically thin and therefore appears shorter and more collimated, exactly what we see in IRS 1, see Fig 2. For a uniformly expanding spherical wind, the size of the source varies as a function of frequency as $\nu^{-0.7}$, while the flux density density goes as $\nu^{0.6}$ (Panagia & Felli 1975). Since we resolve the emission from IRS 1, we know that it is not spherical, but instead it appears to originate in an initially collimated bipolar jet (opening angle $\lesssim 30^\circ$) approximately aligned with the molecular outflow from IRS 1, see Section 4. For a collimated ionized jet, Reynolds (1986) showed that it can have a spectral index anywhere between 2 and -0.1 , depending on gradients in jet width, velocity, degree of ionization, and temperature.

4. OUTFLOW AND ACCRETION

Although the molecular outflow from IRS 1 in early studies was found to be quite compact and going from SE to NW (Scoville et al. 1986), we find that the molecular outflow is very extended ($> 4'$) and approximately aligned with the free-free jet from analyzing large mosaics obtained with CARMA in ^{12}CO and ^{13}CO $J = 1 \rightarrow 0$, and HCO^+ $J = 1 \rightarrow 0$. For HCO^+ we filled in missing zero spacing with fully sampled single dish maps obtained with FCRAO. A thorough discussion of the molecular outflow is beyond the scope of this paper, and will be discussed in a forthcoming paper (Corder et al. 2009, in prep). Here we therefore summarize some of the main results. The CARMA mosaics show that the

² The emission from IRS 2 is already optically thin at 4.8 GHz (C-band) with an integrated flux of 1440 mJy.

TABLE 1
 OBSERVATIONAL PARAMETERS AND RESULTS OF VLA ARCHIVE DATA OF IRS 1

Frequency [GHz]	Synthesized beam " × " pa = °	rms [mJy beam ⁻¹]	Size bipolar core " × " pa = °	flux density bipolar core [mJy]	flux density total [mJy]	Observing dates
4.86	0.43 × 0.37 + 5.4°	0.30	1.06 × 0.44 -9.6	94.3 ± 4.8	122.5	1984:1123
8.46	1.21 × 0.47 - 0.5°	0.05	0.76 × 0.30 -10.9	135.7 ± 13.6 ^a	148.1 ^a	2003:1014
14.94	0.14 × 0.12 +47.6°	0.017	0.44 × 0.20 -0.3	185.9 ± 5.6	248.7	2006:0226,0512 ^b
14.91	0.14 × 0.10 +13.7°	0.081	0.50 × 0.20 -1.2	165.2 ± 13.3	291.0	1994:1123
22.37	0.08 × 0.08 -43.0°	0.017	0.34 × 0.17 +3.1	286.5 ± 11.5	370.0	1994:1123
43.37	0.14 × 0.12 +14.5°	0.17	0.20 × 0.14 -1.0	429.7 ± 12.9	473.7	2006:0706,0914 ^b

^a Insufficient spatial resolution, blends in with IRS 2. Unreliable total flux.

^b Average of two data-sets at different epochs during the same year.

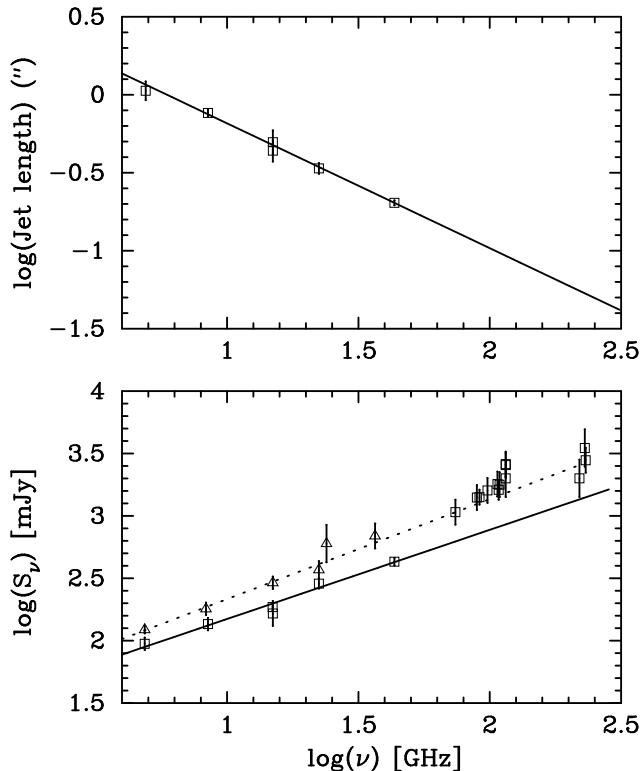


FIG. 3.— *Top panel:* A least squares power-law fit to the length of the optically thick jet as a function of frequency ν gives $\theta(\text{arcsec}) = 4.13 \nu^{-0.8}$ where ν is in GHz. *Bottom panel:* Least squares fit to VLA data (open squares) of the compact bipolar core surrounding IRS1 plotted as a solid line, and to total fluxes (open triangles) plotted with a dotted line. In the figure we also show mm data points obtained with BIMA and CARMA as well as interferometer data from the literature, but they are not used in any of the fits. This plot clearly demonstrates that the free-free emission still dominates the emission in high angular resolution interferometer data even at 1.3 mm.

outflow is very large and has a position angle (pa) of $\sim -20^\circ$, which is similar to the orientation of the collimated inner part of the ionized jet driven by IRS1 on smaller angular scales. The outflow extends several arcminutes to the north and starts as a wide angle limb brightened flow. To the south the outflow is difficult to trace, because of several other outflows in the giant molecular core in which IRS 1 is embedded, but appears more collimated with a linear extent of $\sim 2'$. Analysis of Spitzer IRAC archive data show that the outflow may be even larger to the south. The 5.8 and 8.0 μm IRAC images show a jet-like feature projecting back towards IRS 1, extending

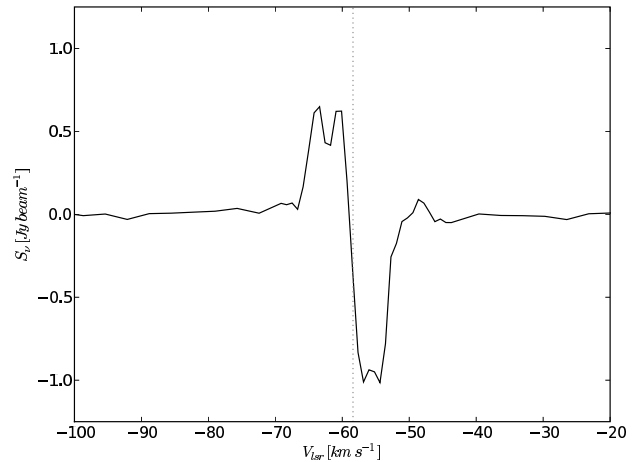


FIG. 4.— Inverse P Cygni profile in $\text{HCO}^+ J = 1 \rightarrow 0$ observed with CARMA supplemented with FCRAO single dish data (Corder 2008). Note that the spectrum is extracted from a continuum subtracted spectral line cube, hence the flux density appears to go below zero. The angular resolution is $4''.5$. The vertical dotted line shows the systemic velocity of IRS 1.

to $\sim 3.5'$ (2.6 pc) from IRS 1, which is much further out than what was covered by the CARMA mosaics (Corder 2008). However, the CARMA observations also confirm that IRS 1 is still heavily accreting. In $\text{HCO}^+ J = 1 \rightarrow 0$ we observe a clear inverse P Cygni profile towards the strong continuum emission from IRS 1 (Fig 4). The absorption is all red-shifted and has two velocity components, which could mean that the accretion activity is varying with time (episodic). From these data Corder (2008) estimates $\sim 6.8 M_\odot$ of infalling gas. With the assumption that the accretion time is similar to the free-fall time, $\sim 30,000$ yr, Corder finds an accretion rate $\sim 2 \cdot 10^{-4} M_\odot/\text{yr}$, which will block most of the uv photons from the central O-star, allowing them to escape only at the polar regions.

5. MILLIMETER DATA - WHERE IS THE ACCRETION DISK?

In Fig. 3 we also plotted flux densities at 3 and 1 mm from the literature (Lugo, Lizano & Garay 2004), supplemented with our own results at 3 mm from BIMA (Wright et al. 2009, in prep) and CARMA (Corder 2008). All the observed flux densities at 3 mm or even at 1.3 mm can be explained by free-free emission, with at most a marginal excess from dust emission. High angu-

lar resolution CARMA continuum observations at 91.4 and 108.1 GHz confirm what is predicted from the fit to total flux densities in Fig 3, i.e. that the free-free emission dominates at 3 mm. These CARMA observations resolve IRS 1 with a size of $0''.5 \times \leq 0''.3$ pa -1° and $0''.4 \times \leq 0''.1$ pa 20° at 94 and 109 GHz, respectively, i.e. the 3 mm emission is aligned with the free-free emission, and not with an accretion disk, which is expected to be perpendicular to the jet. Since we detect a collimated free-free jet and since there is a strong accretion flow towards IRS 1 (Section 4), IRS 1 must be surrounded by an accretion disk. The morphology of the free-free emission suggests that the disk should be almost edge-on, and centered halfway between the northern and the southern peak of the optically thick inner part of the free-free jet. However, if such an edge-on accretion disk is thin, i.e. the height of the disk is small relative to its diameter, it may not provide much surface area, and is therefore difficult to detect at 3 mm. At 3 mm IRS 1 and IRS 2 are very strong in the free-free, and even the free-free emission from IRS 3 cannot be ignored, which makes it very hard to detect dust emission from the accretion disk. Since the spectral index for dust is $\sim 3 - 3.5$, the dust emission may start to dominate at frequencies above 300 GHz, observable only by SMA, but even at 1.3 mm we may have a much better chance to detect the accretion disk. There is some evidence for such a disk in 450 and 350 μm continuum images obtained at JCMT (Sandell & Sievers 2004). Until higher spatial resolution interferometer images are available, it is not clear whether this emission originates in a disk, from the surrounding in-falling envelope, or from a superposition of several nearby sources.

6. DISCUSSION AND CONCLUSIONS

Free-free emission from ionized jets is very common in low mass protostars (Class 0 and Class I sources), which all appear to drive molecular outflows. This situation is especially true for young stars, which often have rather well collimated outflows (Rodríguez, Anglada & Curiel 1999). Jets may also be common in young early B-type high mass stars (Gibb & Hoare 2007), although they have not been studied as well as low-mass protostars, because they are short lived, more distant and harder to identify. Although there have not been any detections of jets in young O stars, i.e. stars with a luminosity of $> 10^5 L_\odot$, such objects are likely to exist. Broad radio recombination line (RRL) objects, many of which are classified as Ultra Compact or Hyper Compact H II regions (Jaffe & Martín-Pintado 1999; Kurtz & Franco

2002; Sewilo et al. 2004; Keto et al. 2008) offer a logical starting point, because they show evidence for substantial mass motions, which would be readily explained if the recombination line emission originates in a jet. Several of them also show evidence for accretion. In the sample analyzed by Jaffe & Martín-Pintado (1999), which partly overlaps with the sources discussed by Gibb & Hoare (2007), they find four sources (including IRS 1) with bipolar morphology. All appear to be dominated by wind ionized emission, although not necessarily jet driven winds. K 3-50 A, however, at a distance of 8.7 kpc (De Pree et al. 1994), has a luminosity of a mid-O star, drives an ionized bipolar outflow (De Pree et al. 1994), and has a spectral index of 0.5 in the the frequency range 5 - 15 GHz (Jaffe & Martín-Pintado 1999). K 3-50 A is therefore another example of an O-star, where the free-free emission appears to be coming from an ionized jet. Detailed studies of broad RRL objects will undoubtedly discover more examples of jet-ionized H II regions. Such objects are likely to drive molecular outflows, excite masers and show evidence for strong accretion.

To summarize: We have shown that the emission from IRS 1 is completely dominated by a collimated ionized jet. The jet scenario also readily explains why the free-free emission is variable, because the accretion rate from the surrounding clumpy molecular cloud will vary with time. It also explains why IRS 1 is an extreme broad RRL object. Since most Hyper Compact H II regions are broad RRL objects, and show rising free-free emission with similar spectral index to IRS 1, other sources now classified as Hyper Compact H II regions, may also be similar to IRS 1.

The National Radio Astronomy Observatory (NRAO) is a facility of the National Science Foundation operated under cooperative agreement by Associated Universities, Inc. The BIMA array was operated by the Universities of California (Berkeley), Illinois, and Maryland with support from the National Science Foundation. Support for CARMA construction was derived from the states of California, Illinois, and Maryland, the Gordon and Betty Moore Foundation, the Kenneth T. and Eileen L. Norris Foundation, the Associates of the California Institute of Technology, and the National Science Foundation. Ongoing CARMA development and operations are supported by the National Science Foundation under a cooperative agreement, and by the CARMA partner universities.

REFERENCES

- Campbell, B. 1984, *ApJ*, 282, L27
 Corder, S. 2008, PhD thesis, Caltech
 De Pree, C. G., Goss, W. M., Palmer, P., & Rubin, R. H. 1994, *ApJ*, 428, 670
 Franco-Hernández, R., & Rodríguez, L. F. 2004, *ApJ*, 604, L105
 Gaume, R. A., Goss, W. M., Dickel, H. R., Wilson, T. L., and Johnston, K. J. 1995, *ApJ*, 438, 776
 Gibb, A. G., & Hoare, M. G. 2007, *MNRAS*, 380, 246
 Hackwell, J. A., Grasdalen, G. L., and Gehr, R. D. 1982, *ApJ*, 252, 250
 Jaffe, D. T., & Martín-Pintado, J. 1999, *ApJ*, 520, 162
 Keto, E., Zhang, Q., & Kurtz, S. 2008, *ApJ*, 672, 423
 Kurtz, S., & Franco, J. 2002, *RevMexAA*, 12, 16
 Lugo, J., Lizano, S., & Garay, G. 2004, *ApJ*, 614, 807
 Martin, A. H. M. 1973, *MNRAS*, 163, 141
 Moscadelli, L., Reid, M. J., Menten, K. M., Brunthaler, A., Zheng, X. W., & Xu, Y. 2008, [astro-ph]arXiv:0811.0679v1
 Panagia, N. & Felli, M. 1975, *A&A*, 39, 1
 Reynolds, S. P. 1986, *ApJ*, 304, 713
 Rodríguez, L. F., Anglada, L., & Curiel, S. 1999, *ApJS*, 125, 427
 Sandell, G., Goss, W. M., & Wright, M. 2005, *ApJ*, 621, 839
 Sandell, G., & Sievers, A. 2004, *ApJ*, 600, 269
 Sewilo, M., Churchwell, E., Kurtz, S., Goss, W. M., & Hofner, P. 2004, *ApJ*, 605, 285
 Scoville, N. Z., Sargent, A. I., Claussen, M. J., Masson, C. R., Lo, K. Y., & Phillips, T. G. 1986, *ApJ*, 303, 416
 Wynn-Williams, C. G., Becklin, E. E., and Neugebauer, G. 1974, *ApJ*, 187, 473